THE JOURNAL OF PHYSICAL CHEMISTRY C
A JOURNAL OF THE AMERICAN CHEMICAL SOCIETY

pubs.acs.org/JPCC

Article

How Nitrogen Doping Affects Hydrogen Spillover on Carbon-Supported Pd Nanoparticles: New Insights from DFT

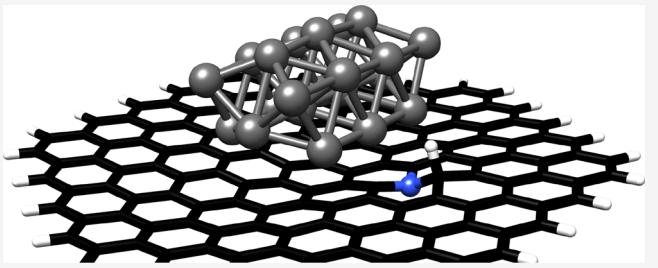
Lisa Warczinski* and Christof Hättig

Cite This: https://doi.org/10.1021/acs.jpcc.0c11412

Read Online

ACCESS | Metrics & More | Article Recommendations | Supporting Information

ABSTRACT: The process of hydrogen spillover on metal nanoparticle decorated carbon surfaces has been discussed for many years due to its importance for heterogeneous catalysis and hydrogen storage. The present density functional theory (DFT) study supports recent experimental observations of the hydrogen spillover process. By use of model systems of carbon-supported palladium nanoparticles, the details of hydrogen spillover are investigated and the effects of nitrogen doping on such processes are elucidated. It is found that graphitic nitrogen atoms and water molecules significantly facilitate the hydrogen spillover reaction and serve as anchoring sites for the spillover hydrogen atoms.



Downloaded via BOCHUM LIBRARIES on April 22, 2021 at 06:12:22 (UTC).
See https://pubs.acs.org/sharingguidelines for options on how to legitimately share published articles.

INTRODUCTION

In a hydrogen spillover process, activated hydrogen species adsorbed or formed on a first surface are moved to a second surface on which, under the same conditions, these activated hydrogen species could not adsorb or form.[1] For the first time, the hydrogen spillover effect was reported in 1964 by Khoobiar, who observed a transport of hydrogen atoms from Pt to WO_3.[2] In the past decade, hydrogen spillover from metal nanoparticles onto carbon materials has attracted tremendous attention as the spillover effect significantly enhances the carbon material's capability of storing hydrogen.[3−7] This opens up the possibility of using metal nanoparticle decorated carbon materials as hydrogen storage in future fuel cell systems. Also the usage of reversibly stored spillover hydrogen for heterogeneous catalyzed reactions, e.g., for hydrogenation reactions, is of high interest.[8]

Up to the present, several experimental studies have tried to shed light on the details of the hydrogen spillover mechanism, which turned out to be quite difficult due to the complicated characterization of the carbon support and the hydrogen spillover species.[2] In recent years, Li et al.[9] and Wang et al.[10] observed that surface functional groups and residual moisture significantly enhance the spillover process. In a comprehensive study on hydrogen spillover on platinum/nitrogen-doped mesoporous carbon (NMC) composites from the year 2018, Yang et al.[8] provided novel insights into the hydrogen spillover effect. They were able to generate and to give experimental evidence of spillover hydrogen on the nitrogen-doped carbon support material. Furthermore, they characterized spillover hydrogen as a mobile and reversibly stored hydrogen species, present in a chemically inactive state. On the basis of these observations, they suggested that spillover hydrogen is adsorbed as protons on the carbon support material, which might be further stabilized by water molecules.

In general, it is very difficult to detect spillover hydrogen species in experiments.[1,11,12] Several experimental results on the hydrogen spillover effect were later proven to be erroneous.[2] Therefore, the purpose of the present study is to use quantum chemistry to support the recent experimental observations[8−10] and to improve the understanding of the hydrogen spillover process and of the properties of spillover hydrogen. We particularly aim to shed light on the effect of different nitrogen functional groups on the properties of spillover hydrogen and to elucidate how nitrogen doping could enhance the hydrogen spillover on carbon-supported metal nanoparticles. Furthermore, we study the interaction of spillover hydrogen atoms with water molecules, which on the real catalysts are difficult to avoid and might play a crucial role for spillover hydrogen. For our study, we apply density functional theory (DFT) to models of mesoporous carbon supported palladium nanoparticles, in which a Pd_{21} cluster is supported on a hydrogen terminated graphene layer. As we have shown that graphitic nitrogen (6% relative abundance in the NMC support material) and pyridinic nitrogen species (45% relative abundance in the NMC support material) significantly tune the properties of the anchored Pd nano-

Received: December 23, 2020
Revised: March 21, 2021

ACS Publications

© XXXX The Authors. Published by American Chemical Society

particles in a previous study,[13] the nitrogen doping is modeled by incorporated graphitic and pyridinic nitrogen atoms.

Similar approaches have been used in several studies and have provided valuable insights into the properties of carbon-supported Pd nanoparticles. However, most of these studies used single Pd atoms or very small Pd clusters.[14−16] As an example, Rangel et al.[17] investigated the hydrogen spillover process on Pd_4 clusters. One of our previous studies[18] has demonstrated that it is essential to also consider larger cluster sizes like Pd_{21}, which are closer to Pd nanoparticle sizes present in experimental systems. Several aspects of hydrogen adsorption, dissociation, and diffusion on clean and doped graphitic surfaces have been studied before both theoretically and experimentally; e.g., see refs 19 and 20 and the recent review[21] by Gerber et al. In the current work we study the effects of doping a graphitic surface with chemically different nitrogens on the spillover from Pd nanoparticles together with binding and diffusion of the spillover hydrogen and provide additional insights into the electronic structure of hydrogen at the different binding sites.

The experimentally observed hydrogen spillover is a complex multistep process, influenced by several aspects as hydrogen pressure, temperature, impurities, and catalyst morphology. The experimental catalyst systems, Pd nanoparticles on nitrogen-free mesoporous carbon, Pd/CMC, and Pd/NMC, include surface deformations, further defects like five- and seven-membered rings, or surfactants and residual moisture. As studying all these aspects at the same time would introduce too many degrees of freedom, the present study utilizes model systems and deals with the different steps of the hydrogen spillover process separately. As a consequence, we focus on qualitative observations and do not compare our results to specific experimental values. Elucidating the energetics of the individual steps constitutes an important step toward a better understanding of hydrogen spillover and of the effect of nitrogen doping on such processes. Furthermore, the present study can give some computational evidence if hydrogen could actually be reversibly stored on Pd/NMC.

COMPUTATIONAL DETAILS

Model Systems. To model the nitrogen-free mesoporous carbon support material (CMC), we chose a hydrogen terminated graphene layer comprising 96 carbon atoms (see Figure 1). In nitrogen-doped mesoporous carbon the nitrogen atoms can be present in four forms: graphitic N, pyridinic N, pyrrolic N, and N−O like species.[13] As pyrrole-like and N−O-like nitrogen atoms are either located on the edges of the support material or include large surface deformations, both of which would introduce undesired side effects in the electronic structure calculations of the reactions, these systems have not been considered. Accordingly, to model the NMC support material, one (graphitic N, see Figure 2a) or three (pyridinic N, see Figure 2b) carbon atoms of the graphene layer were replaced by nitrogen atoms.

To model the carbon-supported palladium nanoparticles (Pd/CMC), we chose a Pd_{21} cluster supported by a hydrogen terminated graphene layer of 150 carbon atoms (see Figure 3). The Pd_{21} cluster possesses a diameter of around 0.85 nm, corresponding to sizes at the lower boundary of experimentally determined particle size distributions for Pd/CMC and Pd/NMC, which show nanoparticles of 1−8 nm as well as some sub-1 nm Pd particles.[22] This cluster, which has before been

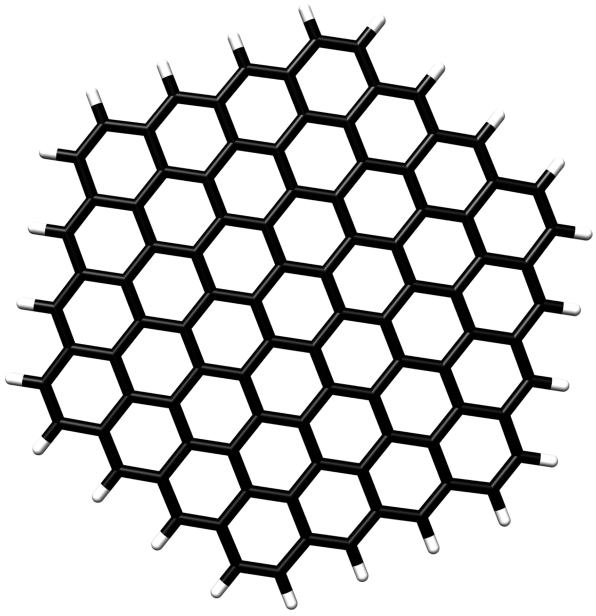


Figure 1. Model system for the pure mesoporous carbon support material (CMC).

successfully used to study hydrogen adsorption on carbon-supported Pd nanoparticles,[18] was chosen because the upper face atoms reflect a Pd {111} facet and possesses two adjacent face centered cubic (fcc) sites at the top. Its initial geometry was taken from Shamsiev et al.[23]

Again, for the nitrogen-doped systems (Pd/NMC) one or three carbon atoms were replaced by nitrogen atoms to model, respectively, graphitic or pyridinic N-sites. The configurations of Pd_{21} on the supports with graphitic and pyridinic N for the present study are shown in Figure 4. The Pd_{21} cluster has been validated in previous investigations. In a study on hydrogen absorption on carbon-supported Pd nanoparticles[18] it turned out as a suitable model for the metal−support interaction between Pd nanoparticles and the carbon support and its influence on hydrogen adsorption. The models for the nitrogen-doped support were evaluated in a combined theoretical and experimental study on the anchoring of Pd nanoparticles at nitrogen defects in NMC[13] and later applied in a study of the bifunctional catalytic role of Pd/NMC for the reduction of 5-hydroxymethylfurfural.[22] For further details we refer the readers to refs 13, 18, and 22 and the Supporting Information provided with these studies.

METHODOLOGY

The present density functional theory (DFT) study was performed using the TURBOMOLE[24] program package with the TPSS[25] functional and the def2-SVP[26] basis set. Stuttgart−Cologne 28-electron effective core potentials (def2-ecp)[27] were used for the Pd atoms. All calculations included the multipole accelerated resolution of identity (MARI-J)[28] approximation with optimized auxiliary basis sets[29] and Grimme's D3[30] correction for London dispersion interactions. The most stable structures of our model systems as well as the minima of hydrogen on these systems were determined by ground-state geometry optimizations. To obtain accurate relative energies, single point energies were combined with zero-point vibrational energies (ZPVEs) from vibrational analysis.

https://doi.org/10.1021/acs.jpcc.0c11412
J. Phys. Chem. C XXXX, XXX, XXX−XXX

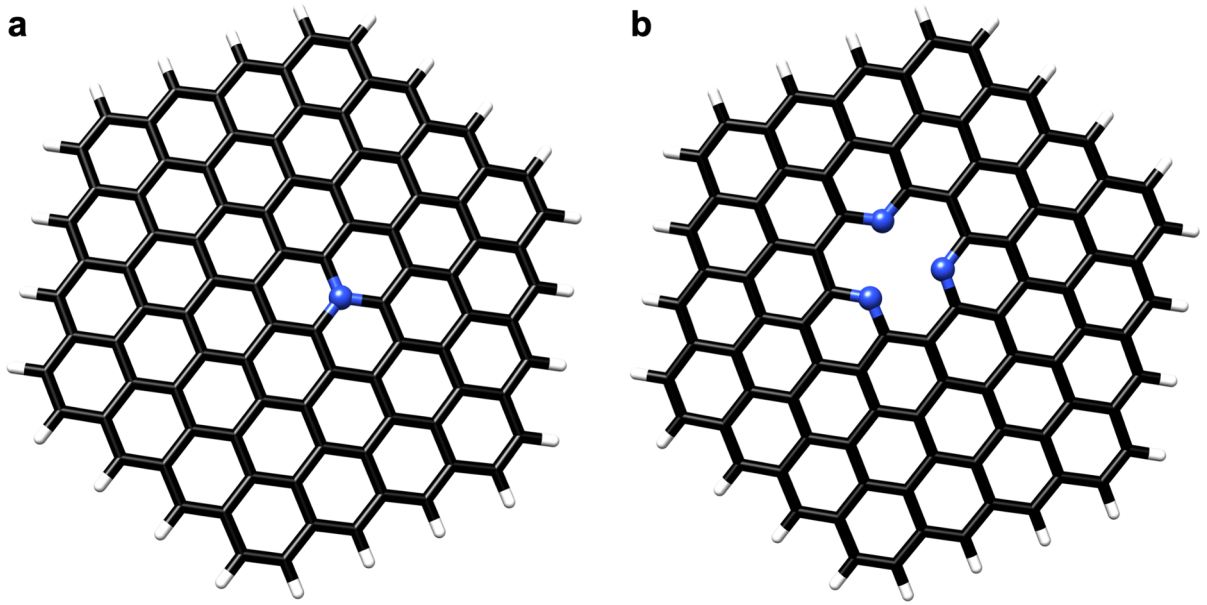


Figure 2. Model systems for the nitrogen-doped mesoporous carbon support material (NMC): (a) graphitic N support; (b) pyridinic N support.

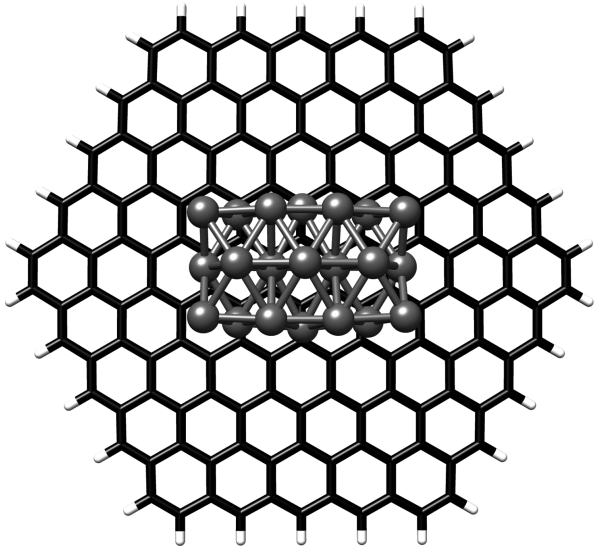


Figure 3. Model system for Pd on the mesoporous carbon support material (Pd/CMC). Adapted from ref 13 with permission from the PCCP Owner Societies.

At this level, results from DFT with different functionals and basis sets can differ in the range of some kJ mol^{-1} per bond. In a previous study[18] we have shown that moving to a larger basis set or to other DFT functionals does affect the DFT energetics of the catalyst systems, but calculated energy differences are similar and the observed trends of the energy differences are essentially the same. Due to the limited comparability of our idealized model systems to experimental catalysts, we anyway limit our conclusions to qualitative observations and omit comparisons to specific experimental values. Our choice of the meta-GGA TPSS functional and the def2-SVP basis set has been shown to be reasonable in several previous studies, as it shows a very good cost/performance ratio for the systems under consideration.[13,18,22,31,32] A comparison of some exemplary TPSS/def2-SVP energy differences with those from PBE/def2-SVP and TPSS/def2-TZVP on the basis of TPSS/def2-SVP geometries, which document the good agreement of energetics calculated with different functionals and basis sets for our systems, can be found in the Supporting Information (see Tables S1−S3).

Reaction pathways were predicted using the chain-of-state method implemented in the woelfling module of TURBOMOLE,[33] and the found initial transition state structures were then further optimized with the trust-region image minimization (TRIM)[34] algorithm. All transition states were finally validated by intrinsic reaction coordinate (IRC)[35] calculations. To allow for a qualitative comparison of the calculated results to experimental studies, Gibbs free reaction enthalpies and free activation enthalpies were determined within the harmonic oscillator and rigid rotor approximation under reaction conditions of 473.15 K and 0.1 MPa (chosen analogously to the experimental reaction conditions in ref 8) with a scaling factor of 1.0190 for the TPSS functional.[36] Favorable adsorption energies and dissociation energies are provided with a negative sign, and energy barriers like activation barriers are provided with a positive sign. To arrive at a deeper understanding of the relevant metal−support, hydrogen−support, and metal−hydrogen interactions, we studied intrinsic bond orbitals (IBOs),[37] intrinsic atomic orbital (IAO) charge analyses,[37] and electron density differences. As the π-system of the different support materials can be described well by Hückel theory (see Figure S1 for a validation of Hückel vs DFT), we had a closer look at Hückel orbital energies and population analysis. To model the molecular system after spillover of hydrogen to the support materials within the Hückel theory, the carbon atom attached to the spillover hydrogen was deleted from the π-system.

RESULTS AND DISCUSSION

Electronic Properties of Spillover Hydrogen. As a first step, we investigated the electronic properties of spillover hydrogen. When a hydrogen atom spills over to the carbon support material, it binds to one carbon atom. In this configuration the corresponding carbon atom comes out of the support plane and changes its hybridization partially from

https://doi.org/10.1021/acs.jpcc.0c11412
J. Phys. Chem. C XXXX, XXX, XXX−XXX

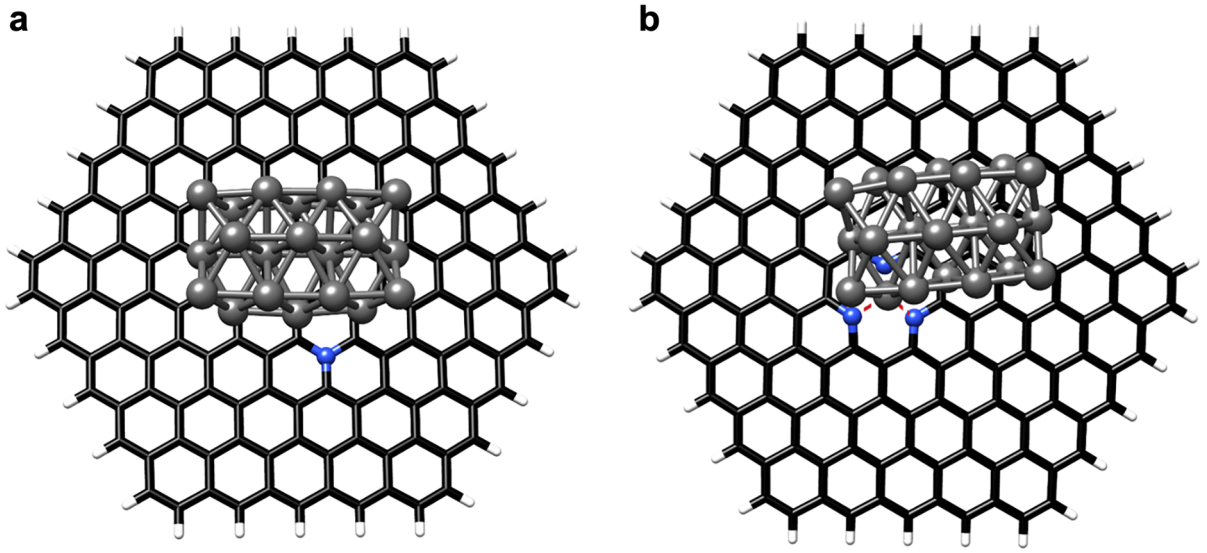


Figure 4. Model systems for Pd on the nitrogen-doped mesoporous carbon support material (Pd/NMC): (a) Pd on graphitic N support; (b) Pd on pyridinic N support. Adapted from ref 13 with permission from the PCCP Owner Societies.

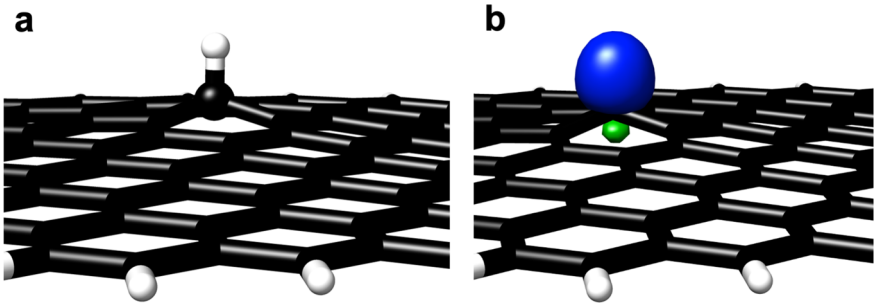


Figure 5. Spillover hydrogen on the graphene support material: (a) geometry; (b) IBO for the C−H bond composed of a C sp^3 hybrid and a H s orbital. Isosurface value is ±0.09.

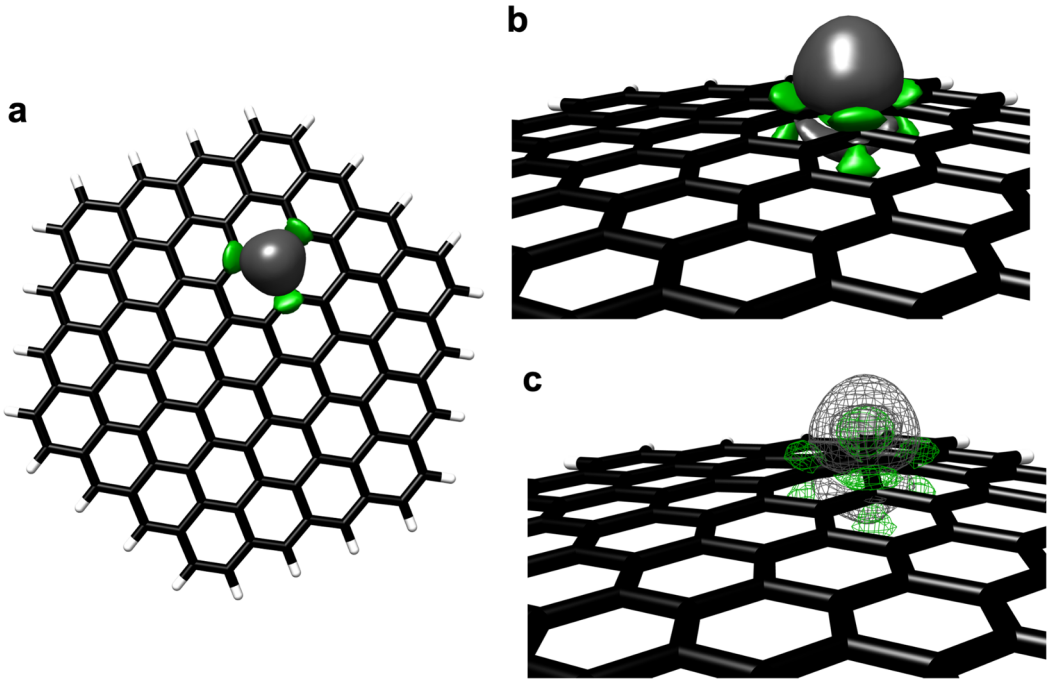


Figure 6. Electron density difference plot for spillover hydrogen on the graphene support material: (a) top view; (b) side view; (c) side view represented with a mesh to reveal inside changes. Density gain is colored in green; density loss is colored in gray. Isosurface value is ±0.0025.

https://doi.org/10.1021/acs.jpcc.0c11412
J. Phys. Chem. C XXXX, XXX, XXX−XXX

sp^2 to sp^3 (see Figure 5a). Consequently, the intrinsic bond orbital (IBO) analysis shows an sp^3 hybrid C−H bonding orbital (see Figure 5b).

Besides the local change of the carbon support geometry, also the electronic structure of the support material is affected as the carbon atom attached to the spillover hydrogen does not contribute to the π-system any more. Accordingly, the spillover hydrogen disturbs the π-system of the support material, which leads to a very unfavorable H_2 dissociation free enthalpy (H_2 + 2CMC → 2H-CMC) of ΔG_{diss} = +362.0 kJ mol^{-1}.

The perturbing effect of spillover hydrogen on the π-system can further be validated with Hückel molecular orbital theory which allows, via a comparison with DFT results, separation of qualitative effects originating from the resonance energy of the π-system from those resulting from other sources as e.g. geometric strain. The Hückel orbital energies show that the spillover hydrogen shifts the highest occupied molecular orbital (HOMO), containing an unpaired electron, up to the Fermi-level (see Figure S2a).

To get further insight into the properties of spillover hydrogen itself, we calculated the electron density difference for spillover hydrogen on the graphene support material (see Figure 6). Like the IBO analysis, the electron density difference plot also proposes that a chemical bond between the spillover hydrogen and one carbon atom is formed as an electron density shift from the π-bonds of the bound carbon atom to an sp^3 hybrid C−H bonding orbital can be observed. Moreover, the plot shows that electron density is shifted from the H s orbital to the π orbitals of the surrounding C atoms. This suggests that spillover hydrogen is positively charged. On the basis of IAO atomic charge analyses, we found that the partial charge of spillover hydrogen (q = +0.16) is more positive than the partial charge of hydrogen atoms located at the edge of the support material or of the hydrogen atoms in the methane molecule (both q = +0.13).

In contrast to the suggestion of Yang et al.,[8] we do not find the spillover hydrogen in the state of a "real" proton, as the electron of the spillover hydrogen atom is localized in an sp^3 hybrid C−H bonding orbital with the H nucleus located at a position where the electron density is higher than for an isolated H atom (see Figure 6c). However, spillover hydrogen atoms possess a relatively high positive partial charge due to electron density shifted from the H s orbital to the π-system.

Furthermore, we studied the effect of nitrogen doping on the properties of spillover hydrogen. Doping with pyridine-like nitrogen atoms slightly increases the positive Gibbs free enthalpy for the H_2 dissociation (for a spillover hydrogen next to the pyridinic N) to ΔG_{diss} = +364.8 kJ mol^{-1}. As the electronegative character of the pyridinic N leads to a positive charge at the neighboring carbon atoms, one would expect that doping with pyridine-like nitrogen atoms would more significantly hinder the binding of a hydrogen radical. However, the higher structural flexibility at the defect allows for geometrical deformations of the support and, therefore, allows for a H−C bond with a stronger sp^3 character, which compensates for the unfavorable electronic effect of the pyridinic N.

In contrast to doping with pyridinic nitrogen, doping with a graphitic nitrogen atom significantly decreases the free enthalpy for the dissociation of H_2 to ΔG_{diss} = +150.4 kJ mol^{-1} if the H atom is bound at the most favorable site, which is the C atom in ortho position to the nitrogen. This observation is again explained by the resonance energies for the π system. The graphitic nitrogen atom possesses an additional (in comparison to C) electron in the π-system, which is unpaired and facilitates the binding of a hydrogen radical. This can be validated with the Hückel orbital energies, which show a highest occupied molecular orbital (HOMO) doubly occupied and significantly below the Fermi-level (see Figure S2b). Furthermore, in the electron density difference it can be observed that the graphitic nitrogen atom leads to a delocalization of shifted electron density from the H s orbital to the π-system of the support material (see Figure 7 and Figure S3 for electron density difference plots for systems with two and six graphitic N atoms).

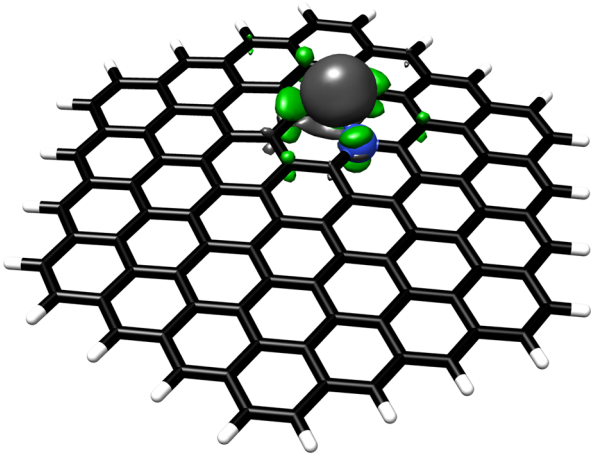


Figure 7. Electron density difference plot for spillover hydrogen on the graphitic N support material. Density gain is colored in green; density loss is colored in gray. Isosurface value is ±0.0025.

It is important to note that the extent of the effect of the graphitic nitrogen atom on the π-system depends on its position with respect to the spillover hydrogen (see Figure 8 for a sketch of the different positions). This effect is almost quantitatively due to the resonance energies of the π-sytem as the comparison of the energy differences obtained at the DFT level with the resonance energies from Hückel theory stabilization energies for the different positions in Table 1

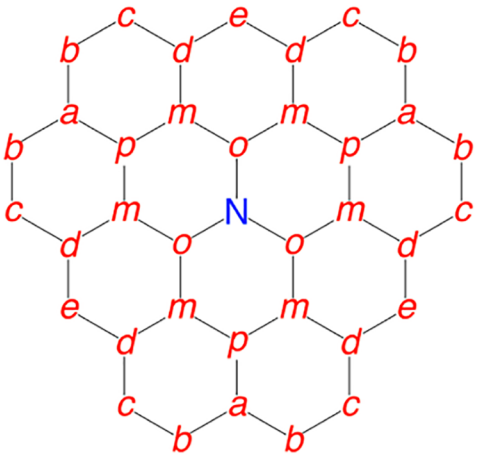


Figure 8. Sketch of spillover hydrogen atom positions on graphitic N-doped graphene support.

https://doi.org/10.1021/acs.jpcc.0c11412
J. Phys. Chem. C XXXX, XXX, XXX−XXX

shows. Positive relative values indicate a lower stabilization energy and, therefore, a smaller effect of the graphitic N.

Table 1. Hückel and DFT Energy Differences for the Different Spillover Hydrogen Positions Sketched in Figure 8 with Respect to the Most Stable Ortho-Position, for Hückel in Units of the Resonance Parameter β and for DFT in kJ mol^{-1}

hydrogen position	Hückel, $\lvert\beta\rvert$	DFT, kJ mol^{-1}
o	0.00	0.0
m	0.51	60.4
p	0.25	19.8
a	0.51	101.4
b	0.42	61.5
c	0.49	80.4
d	0.48	90.6
e	0.50	85.7

The extent of the effect is very similar to arene substitution patterns and can be summarized as follows:

- within first shell: o < p < m
- within second shell: b < d, c, e, a

The decoration of the support material with palladium clusters in general increases the stability of spillover hydrogen atoms as the cluster takes over most of the spin density of the hydrogen radical (see Figure 9). The positive free enthalpy of the H_2 dissociation for a spillover hydrogen atom directly next to a Pd_{21} cluster is reduced to +230.0 kJ mol^{-1} compared to +362.0 kJ mol^{-1} for the pure graphene support system.

Hydrogen Spillover Pathways. As a second step, we investigated the hydrogen spillover process on carbon-supported Pd nanoparticles. In our previous study[18] it was shown that carbon-supported Pd clusters can adsorb and dissociate several hydrogen molecules. In experiments, the Pd cluster is most probably covered with hydrogen before the hydrogen spillover process takes place.

To elucidate the configuration of several chemisorbed hydrogen molecules on the Pd nanoparticles, a geometry of the carbon-supported Pd_{21} cluster loaded with 26 hydrogen atoms was optimized (see Figure 10). The most stable positions of hydrogen atoms on the Pd cluster are triangular positions at the top of the cluster, bridging three palladium

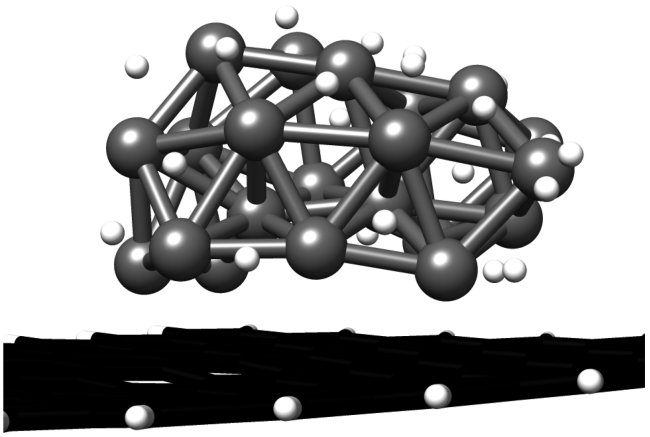


Figure 10. Geometry of carbon-supported Pd_{21} loaded with 26 hydrogen atoms.

atoms (further details can be found in ref 18). When, subsequently, several hydrogen molecules are chemisorbed on the cluster, hydrogen atoms are attached to the side of the cluster and to even less stable bridge positions on top of Pd–Pd bonds. Several studies on Pd crystals suggest that hydrogen could also be absorbed inside the cluster.[38]

We determined the reaction pathways for the hydrogen spillover process from the Pd_{21} cluster to the three different support materials using a model system with (only) one hydrogen atom, which is located in a triangular position at the side of the cluster. This was necessary because the structural flexibility of the Pd cluster with the high hydrogen loading impeded the localization of a proper transition state and the calculation of the vibrational corrections to the activation energy. For the system with the lowest activation energy (Pd_{21}/graphitic N support), also the pathway from a less stable position, in which the H atom bridges a Pd–Pd bond at the bottom of the cluster, was considered. The corresponding pathways for the pure graphene support and the pyridinic N support have not been studied; however, the effect of changing the starting point from the triangle to the bridge position on the energetics should be very similar.

A sketch of the hydrogen spillover reaction pathway from Pd_{21} to the support doped with graphitic N is shown in Figure 11. Figures 12 and 13 show the corresponding pathways on

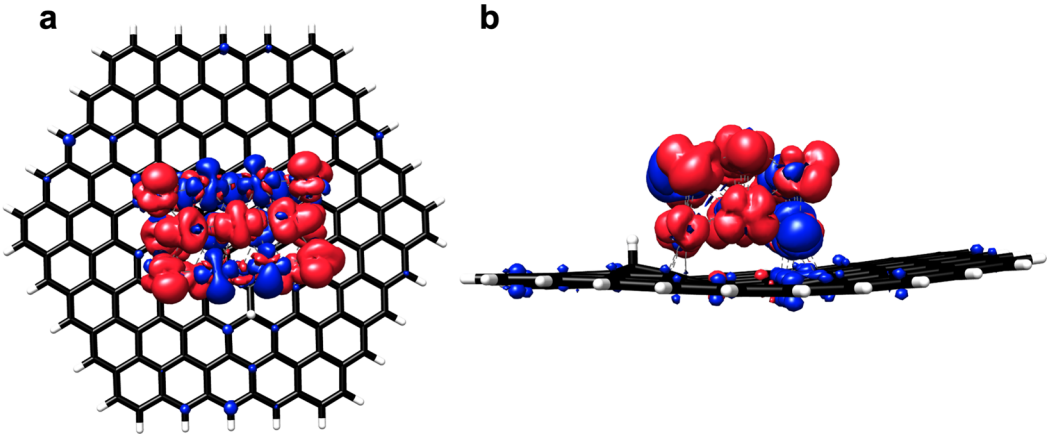


Figure 9. Plot of the spin density for a spillover hydrogen atom located directly next to a Pd_{21} cluster: (a) top view; (b) side view. Isosurface value is ±0.0005.

https://doi.org/10.1021/acs.jpcc.0c11412
J. Phys. Chem. C XXXX, XXX, XXX–XXX

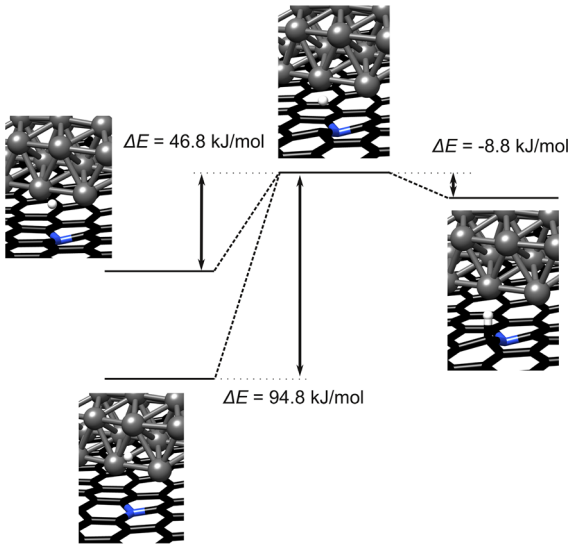


Figure 11. Hydrogen spillover pathway from Pd_{21} to the graphitic N support material from two different initial sites.

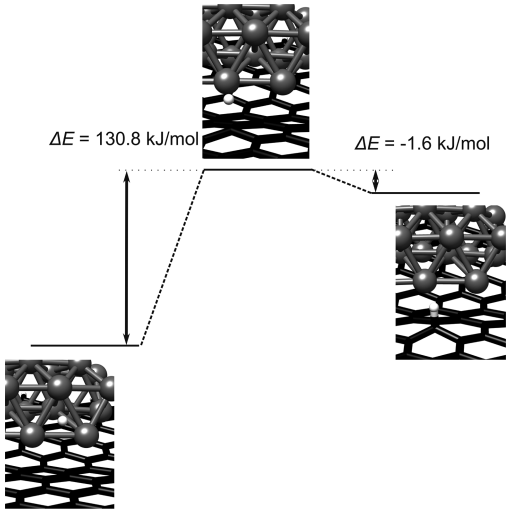


Figure 12. Hydrogen spillover pathway from Pd_{21} to the pure graphene support material.

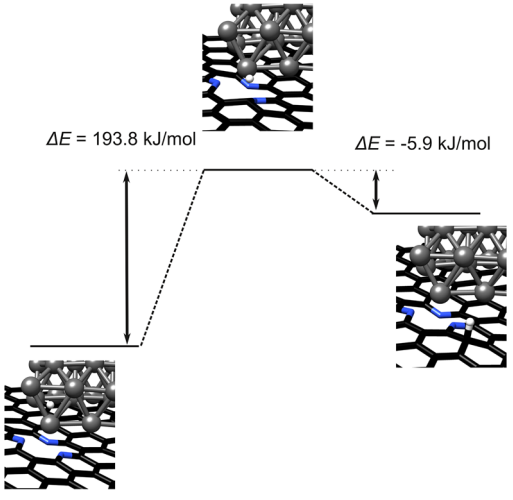


Figure 13. Hydrogen spillover pathway from Pd_{21} to the pyridinic N support material.

graphene and support doped with pyridinic N. Table 2 shows the activation energies (ΔE_{act}) and the free activation enthalpies (ΔG_{act}) for the hydrogen spillover from Pd_{21} on the three different support materials. For the graphitic N support, also the activation energy and free activation enthalpy from the less stable reactant are listed. Table 3 shows the corresponding reaction energies (ΔE_{react}) and free reaction enthalpies (ΔG_{react}).

Table 2. Activation Energies and Free Activation Enthalpies for the Hydrogen Spillover from Pd_{21} onto Different Support Materials

model system	ΔE_{act}, kJ mol^{-1}	ΔG_{act}, kJ mol^{-1}
Pd_{21} on graphene support; triangle site	130.8	140.8
Pd_{21} on graphitic N support; triangle site	94.8	97.9
Pd_{21} on graphitic N support; bridge site	46.8	50.4
Pd_{21} on pyridinic N support; triangle site	193.8	200.3

Table 3. Reaction Energies and Free Reaction Enthalpies for the Hydrogen Spillover from Pd_{21} onto Different Support Materials

model system	ΔE_{react}, kJ mol^{-1}	ΔG_{react}, kJ mol^{-1}
Pd_{21} on graphene support; triangle site	129.2	143.4
Pd_{21} on graphitic N support; triangle site	86.0	94.4
Pd_{21} on graphitic N support; bridge site	38.0	47.0
Pd_{21} on pyridinic N support; triangle site	187.9	187.4

On the pure graphene support material the hydrogen spillover reaction starting from the triangle site shows quite a high activation energy and free activation enthalpy. Even if one assumes that starting from the less stable bridge position will decrease the Gibbs free reaction enthalpy by around 45 kJ mol^{-1} (approximated from the result for the graphitic N system), it still mounts up to around 100 kJ mol^{-1}. This indicates that the hydrogen spillover to pure carbon support materials is kinetically difficult, which is also in agreement with previous ab initio molecular dynamics (AIMD) simulations, which have not found a single case of hydrogen spillover from Pd_6 or Pd_{13} clusters to pure graphene.[39]

Doping with graphitic N atoms significantly decreases the activation energy and free activation enthalpy of the spillover reaction (for the triangle site to around 95 kJ mol^{-1}; for the bridge site to around 50 kJ mol^{-1}). This effect can be explained on the basis of Hammond's postulate: In general, the hydrogen spillover reaction is an endothermic reaction (see Table 3). The transition state is very similar to the product state, which is called "late" transition state. As the doping with graphitic N atoms decreases the positive reaction energy and, therefore, stabilizes the product state (due to its additional electron; see previous section), the doping also stabilizes the transition state.

Analogous to the explanation for the decrease of the activation energy for the graphitic N system, also the increase of the activation energy for the pyridinic N system can be explained using Hammond's postulate. As described in the previous section, the positively charged carbon atoms next to the pyridinic N significantly hinder the binding of the spillover hydrogen. In comparison with the free support material, the binding of the Pd cluster on the surface defect hinders a change of the support geometry upon hydrogen spillover.

https://doi.org/10.1021/acs.jpcc.0c11412
J. Phys. Chem. C XXXX, XXX, XXX−XXX

Accordingly, doping with pyridinic nitrogen destabilizes the product of the hydrogen spillover (see Table 3) and, therefore, also increases the activation energy.

In general, our calculations reveal that the hydrogen spillover is significantly facilitated by graphitic N atoms. The free activation enthalpy for the spillover from the less stable bridge site is only around 50 kJ mol^{-1}. According to the Arrhenius law

$$\nu = \nu_0 \exp\left[\frac{-\Delta E_{act}}{k_B T}\right] \quad (1)$$

with the activation energy ΔE_{act} = 46.8 kJ mol^{-1} and a common estimate of the pre-exponential value of $\nu_0 = \frac{k_B T}{h} = 1 \times 10^7$ s^{-1},[17,40,41] one can expect a hydrogen migration rate of $\nu \sim 7 \times 10^7$ s^{-1} at 473.15 K. This sufficiently high rate gives some evidence that doping with graphitic nitrogen atoms could actually enable the hydrogen spillover process on Pd/NMC, which is also in agreement with the experimental observation of hydrogen spillover on Pt/NMC by Yang et al.[8]

Hydrogen Bonds Formed by Spillover Hydrogen and Water Molecules. To get an insight into the interaction of spillover hydrogen with residual moisture, we optimized the geometry of a water molecule close to spillover hydrogen. The equilibrium geometry indicates that the spillover hydrogen atom somehow interacts with the oxygen atom of the water molecule (see Figure 14). However, the intrinsic bond orbital (IBO) analysis does not give any bonding orbitals between the water O and the spillover H atom. Accordingly, the spillover hydrogen atom is not strongly acidic; i.e. it does not protonate H_2O to form H_3O^+, which is in agreement with our previous findings, showing that spillover hydrogen is positively charged but is not in the state of acidic protons.

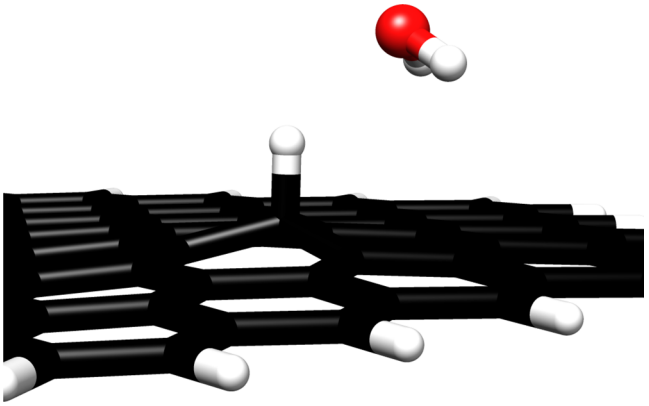


Figure 14. Equilibrium geometry of water on a spillover hydrogen.

To elucidate the details of the C−H−O interaction, we calculated the electron density difference of the spillover hydrogen−water system (see Figure 15a) and compared it to the electron density difference of the water dimer (see Figure 15b). The electron density differences of these two systems are nearly equivalent. This indicates that the previously found positive partial charge of spillover hydrogen is high enough so that it can form hydrogen bonds with water molecules. The energy of such a hydrogen bond is E_{hbond} = −37.0 kJ mol^{-1} at a hydrogen bond length of r_b = 2.24 Å, compared to E_{hbond} = −28.7 kJ mol^{-1} and r_b = 1.90 Å for the water dimer. This is in agreement with the experimental studies of Yang et al.,[8] Li et al.,[9] and Wang et al.,[10] which propose that spillover hydrogen is stabilized by water molecules.

Diffusion of Spillover Hydrogen. To investigate if spillover hydrogen can play a role in hydrogenation reactions and if it lends itself for the purpose of hydrogen storage, it is important to also study the diffusion of spillover hydrogen on the support material. Table 4 lists the activation energies (ΔE_{act}) and the free activation enthalpies (ΔG_{act}) for the diffusion pathways on the three different support materials, which are sketched in Figure 16. Table 5 shows the corresponding reaction energies (ΔE_{react}) and free reaction enthalpies (ΔG_{react}). In all these pathways the spillover hydrogen diffuses in a chemisorbed state from one to the neighboring carbon atom, surpassing a transition state in which the H atom bridges a carbon−carbon bond.

Table 4. Activation Energies and Free Activation Enthalpies for Spillover Hydrogen Diffusion on Different Support Materials

diffusion pathway	ΔE_{act}, kJ mol^{-1}	ΔG_{act}, kJ mol^{-1}
a: on pure graphene support material	105.0	107.6
b: on graphitic N support material	121.5	123.9
c: on pyridinic N support material	45.1	46.9

On the pure graphene support material the chemisorbed diffusion pathway (pathway a) shows a quite high activation energy and Gibbs free activation enthalpy. An IBO analysis and an IAO partial charge calculation reveal that the spillover hydrogen in the transition state is bound to two carbon atoms

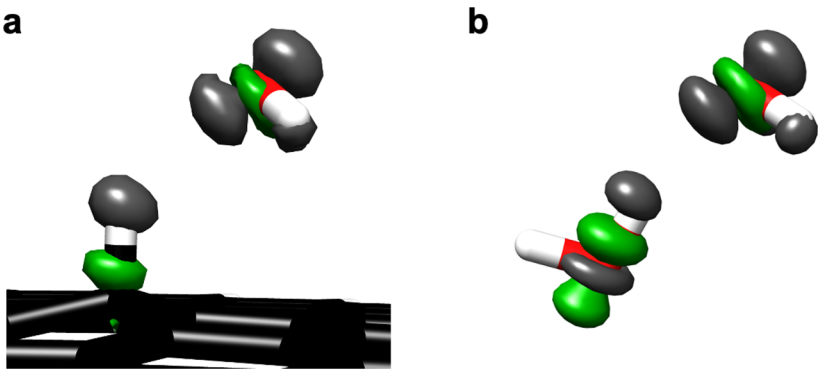


Figure 15. Electron density difference plots: (a) interaction of water with a spillover hydrogen; (b) interaction of the water dimer. Density gain is colored in green; density loss is colored in gray. Isosurface value is ±0.0025.

https://doi.org/10.1021/acs.jpcc.0c11412
J. Phys. Chem. C XXXX, XXX, XXX−XXX

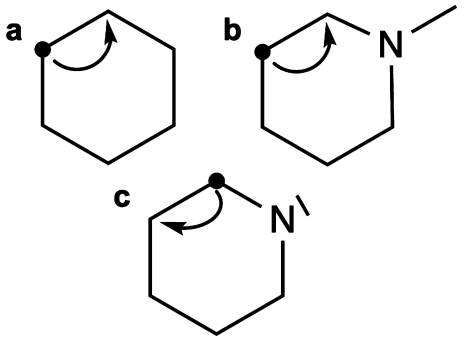


Figure 16. Sketch of spillover hydrogen diffusion pathways: (a) diffusion on pure graphene support material; (b) diffusion on graphitic N support material; (c) diffusion on pyridinic N support material.

Table 5. Reaction Energies and Free Reaction Enthalpies for Spillover Hydrogen Diffusion on Different Support Materials

diffusion pathway	ΔE_{react}, kJ mol^{-1}	ΔG_{react}, kJ mol^{-1}
a: on pure graphene support material	~0.0	~0.0
b: on graphitic N support material	−62.6	−62.3
c: on pyridinic N support material	−53.4	−32.5

and is significantly stronger positively charged compared to spillover hydrogen in the equilibrium geometry (q = +0.25 compared to q = +0.16). Due to the bridging position of the spillover hydrogen, the valence electrons of two carbon atoms are partly taken out of the π-system, which explains the unfavorable energy of the transition state. However, the activation energy and free activation enthalpy of the chemisorbed diffusion pathway can be significantly reduced by a hydrogen bonded water molecule via a Grotthus-like mechanism (ΔG_{act1} = 77.7 kJ mol^{-1}; see Figure S5 and Table S4 for the reaction pathway).

The smallest activation energy and free activation enthalpy can be observed for pathway c, in which the spillover hydrogen atom is located close to a pyridinic nitrogen atom. The found Gibbs free activation enthalpy is only 46.9 kJ mol^{-1}, which corresponds to an expected hydrogen migration rate of $\nu \sim 1 \times 10^8$ s^{-1} at 473.15 K (see eq 1). According to the IBO analysis, the spillover hydrogen in the transition state is solely bound to the carbon atom of the product state. In contrast to the pure graphene support material, it is not symmetrically bound to the two carbon atoms of reactant and product. This effect can be explained by the different charges of the carbon atoms (reactant, positively charged; product, negatively charged), induced by the pyridinic nitrogen dopant. As a consequence, the perturbation of the π-system, and therefore also the activation energy and free activation enthalpy, is significantly lowered.

Close to graphitic N dopants the calculated activation energy and Gibbs free activation enthalpy for the spillover hydrogen diffusion are very high, which is a consequence of its significant spillover hydrogen stabilization. This result indicates that spillover hydrogen will accumulate close to graphitic N atoms in the support material.

When we studied the diffusion of hydrogen spillover to the next but one neighboring carbon atom on the pure graphene support material, we observed that the chemisorbed spillover hydrogen first desorbs via a first transition state to a physisorption minimum, diffuses in this well, and then adsorbs at the next but one neighboring carbon atom, surpassing a second transition state (see Figure 17). According to IBO

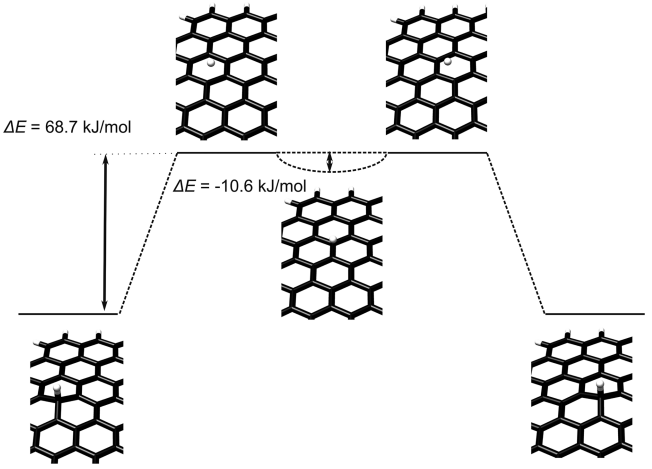


Figure 17. Spillover hydrogen diffusion pathway via a physisorption minimum.

analyses and IAO charge calculations, in both transition states the spillover hydrogen is physisorbed as a hydrogen atom and not bound in a chemisorbed state. In the physisorption minimum the hydrogen atom is in a doublet spin state (the corresponding spin density is shown in Figure S4).

It is important to note that the activation energy and free activation enthalpy for the change of spillover hydrogen from the chemisorbed state to the physisorption minimum are significantly lower compared to the activation energy and free activation enthalpy of the chemisorbed diffusion (ΔE_{act} = 68.5 kJ mol^{-1} and ΔG_{act} = 70.2 kJ mol^{-1} compared to ΔE_{act} = 105.0 kJ mol^{-1} and ΔG_{act} = 107.6 kJ mol^{-1}). This observation is in agreement with previous studies reporting on barrierless diffusion of physisorbed spillover hydrogen atoms.[40,42] Compared to the chemisorbed diffusion, the hydrogen atom in the transition state of the change to the physisorbed state is not chemisorbed at two carbon atoms but only physisorbed at one carbon atom, leading to a smaller perturbation of the π-system and, therefore, to a significantly reduced activation energy and free activation enthalpy. Accordingly, on the pure graphene support material, hydrogen diffusion should occur via a physisorption pathway. The free activation enthalpy for the change of the hydrogen atom from the chemisorbed to the physisorbed state is 70.2 kJ mol^{-1}, which corresponds to an expected rate of $\nu \sim 3.5 \times 10^5$ s^{-1} at 473.15 K (see eq 1).

On the basis of these observations, we also studied the change from the chemisorbed to the physisorbed state for the initial configurations of the nitrogen-doped systems in pathways b and c. The corresponding activation energies and free activation enthalpies for all systems are summarized in Table 6.

Close to a pyridinic N atom the activation energy and free activation enthalpy are slightly higher compared to the pure graphene system, which can be explained with the slightly more stable reactant in the pyridinic system. As the transition state of the chemisorbed diffusion pathway is significantly favored (H atom solely bound to the C atom of the product state), spillover hydrogen diffusion, close to pyridinic N atoms,

https://doi.org/10.1021/acs.jpcc.0c11412
J. Phys. Chem. C XXXX, XXX, XXX−XXX

Table 6. Activation Energies and Free Activation Enthalpies for the Change from the Chemisorbed to the Physisorbed State

model system	ΔE_{act}, kJ mol^{-1}	ΔG_{act}, kJ mol^{-1}
pure graphene support	68.5	70.2
pyridinic N support	80.0	76.3
graphitic N support	107.6	107.4

should occur via a chemisorbed diffusion once H was bound at such a position.

Close to a graphitic N atom the activation energy and free activation enthalpy are significantly higher compared to the pure graphene system. This can also be explained with the high stability of the reactant. Even though the physisorbed diffusion pathway is noticeably facilitated compared to the chemisorbed diffusion pathway (H atom physisorbed at one C atom compared to chemisorption at two C atoms in the transition state), the free activation enthalpy for the change from the physisorbed to the chemisorbed state still mounts up to 107.4 kJ mol^{-1}.

The expected rates of $\nu \sim 1 \times 10^8$ s^{-1} for the hydrogen atom migration in the vicinity of pyridinic nitrogen atoms and of $\nu \sim 3.5 \times 10^5$ s^{-1} for the change from the chemisorbed to the physisorbed state on the pure graphene support material indicate that spillover hydrogen atoms should be mobile on the carbon surface. This was also experimentally proposed by Yang et al.[8] Moreover, spillover hydrogen will accumulate close to graphitic N atoms.

Desorption of Spillover Hydrogen. To further clarify the possible usage of spillover hydrogen in the context of hydrogen storage, also the desorption of two neighboring spillover hydrogens to H_2 has to be considered. Tables 7 and 8

Table 7. Activation Energies and Free Activation Enthalpies for Spillover Hydrogen Desorption on Different Support Materials

support material	ΔE_{act}, kJ mol^{-1}	ΔG_{act}, kJ mol^{-1}
graphene support	232.0	231.2
graphitic N support	128.4	128.3
pyridinic N support	176.8	169.2

Table 8. Reaction Energies and Free Reaction Enthalpies for Spillover Hydrogen Desorption on Different Support Materials

support material	ΔE_{react}, kJ mol^{-1}	ΔG_{react}, kJ mol^{-1}
graphene support	−199.9	−370.2
graphitic N support	−138.4	−194.3
pyridinic N support	−183.8	−243.8

show the activation energies (ΔE_{act}) and free activation enthalpies (ΔG_{act}) as well as the reaction energies (ΔE_{react}) and free reaction enthalpies (ΔG_{react}) of the desorption pathways on the different support materials (see Figures S6, S7, and S8 for the reaction pathways).

It is observed that the spillover hydrogen desorption is highly kinetically hindered on all support materials. On the basis of the previous observation that the change from the chemisorbed to the physisorbed state for spillover hydrogen on the graphene support material shows an activation energy of only 68.5 kJ mol^{-1}, also the hydrogen desorption via an intermediate in which one hydrogen atom is physisorbed should be considered. It is important to note that the change from the chemisorbed to the physisorbed state is significantly hindered by a neighboring hydrogen atom and the activation energy is increased up to 163.2 kJ mol^{-1} for the graphene support system. This can be explained by the fact that the reactant of a chemisorbed spillover hydrogen is stabilized by a neighboring chemisorbed spillover hydrogen atom, as the second hydrogen atom cancels out the radical state of the system. Accordingly, also the hydrogen desorption via a physisorbed intermediate is unfavorable and the formation of spillover hydrogen atom domains is very likely.

Of course, two physisorbed spillover hydrogen atoms coming close together could easily desorb as H_2. However, as the free activation enthalpy for the diffusion from the support material back to the Pd cluster is very small (e.g., 3.5 kJ mol^{-1} for the spillover on the graphitic N support material), spillover hydrogen will rather diffuse back to the Pd cluster than desorb. These results suggest that if hydrogen spillover on Pd/NMC occurs, the spillover hydrogen would be reversibly stored on the carbon support material. This is in agreement with the study of Yang et al.,[8] which gives experimental evidence of reversibly stored spillover hydrogen species on Pt/NMC.

CONCLUSIONS

Using quantum chemistry, we were able to provide an in-depth insight into the hydrogen spillover process on carbon-supported palladium nanoparticles and into the effect of doping with graphitic and pyridinic nitrogen on such processes. We found that the hydrogen spillover reaction is significantly facilitated by graphitic nitrogen atoms, leading to a relatively low Gibbs free activation enthalpy of around 50 kJ mol^{-1} and a feasible migration rate of around 7×10^7 s^{-1} for the spillover of a hydrogen atom from a Pd−Pd bridge position at reaction conditions of 473.15 K and 0.1 MPa. This observation can be explained on the basis of Hammond's postulate as the graphitic nitrogen stabilizes the product state. Diffusion of spillover hydrogen atoms takes place with feasible migration rates at pure graphene support via a physisorbed pathway and in the vicinity of pyridinic nitrogen atoms via a chemisorbed pathway. Close to graphitic nitrogen atoms no diffusion should be observed, as the graphitic nitrogen stabilizes the spillover hydrogen binding due to its additional electron distributed to the π-system. Spillover hydrogen desorption is kinetically hindered on all support materials.

On the basis of these results and the results of our previous study,[13] the following can be concluded: Hydrogen spillover from Pd to pure carbon support materials (as in Pd/CMC) is kinetically difficult. In Pd/NMC the palladium nanoparticles are preferentially anchored on pyridinic nitrogen atoms. Graphitic nitrogen atoms, which make up around 6% of the N functional groups of the NMC surface used in ref 13, significantly reduce the barriers of the hydrogen spillover process. This gives some evidence that graphitic nitrogen atoms could actually enable the hydrogen spillover process on Pd/NMC. The calculated positive Gibbs free reaction enthalpies for all spillover reaction pathways are due to the fact that our calculations just include one hydrogen atom on the cluster. In the chemical equilibrium of a high hydrogen coverage on the supported Pd nanoparticle, as it is present when the hydrogen spillover occurs, ΔG of the hydrogen chemisorption on the Pd cluster should be zero. The calculated free chemisorption enthalpy of H_2 on our model system is on

https://doi.org/10.1021/acs.jpcc.0c11412
J. Phys. Chem. C XXXX, XXX, XXX−XXX

the order of −60 kJ mol^{-1}, which will compensate for the remaining positive free reaction enthalpy of the spillover process. Moreover, in the chemical equilibrium the supported Pd cluster is most probably (after hydrogen spillover) continuously reloaded with hydrogen from the gas phase, which changes the overall reaction equation.

Besides their effect on the spillover process, graphitic and pyridinic nitrogen atoms can serve as anchoring sites where spillover hydrogen species will accumulate. While at graphitic nitrogens we find a rather high barrier for the migration to or away from the carbons in ortho position to the N atoms, the respective barriers are much lower close to pyridinic N atoms.

When the hydrogen spillover process actually occurs on Pd/NMC, the spillover hydrogen will be reversibly stored on the carbon support material as the barriers for migrating back from the carbon support to the Pd nanoparticle are quite small and spillover hydrogen desorption is unlikely.

In general, we do not find that spillover hydrogen is in the state of "real" protons. However, the spillover hydrogen is positively charged and is stabilized significantly by water molecules of residual moisture via hydrogen bonds. These water molecules also reduce the barrier for migration of hydrogen atoms on the carbon support. Via a Grotthus-like mechanism they might enhance considerably the diffusion of spillover hydrogen on CMC and NMC supports.

■ ASSOCIATED CONTENT

Supporting Information

The Supporting Information is available free of charge at https://pubs.acs.org/doi/10.1021/acs.jpcc.0c11412.

Hückel calculations, stability with respect to DFT functional and basis set, electron density differences, spin density, additional reaction pathways, and different energy contributions (PDF)

■ AUTHOR INFORMATION

Corresponding Author

Lisa Warczinski − *Ruhr-University Bochum, 44780 Bochum, Germany;* orcid.org/0000-0002-1884-9251; Email: lisa.warczinski@rub.de

Author

Christof Hättig − *Ruhr-University Bochum, 44780 Bochum, Germany;* orcid.org/0000-0002-5752-2710

Complete contact information is available at: https://pubs.acs.org/10.1021/acs.jpcc.0c11412

Notes

The authors declare no competing financial interest.

■ ACKNOWLEDGMENTS

This work has been supported by the Deutsche Forschungsgemeinschaft within the framework of the Sino-German initiative "Novel Functional Materials for Sustainable Chemistry" through Grant Ha 2588/9-1.

■ REFERENCES

(1) Conner, W. C.; Falconer, J. L. Spillover in Heterogeneous Catalysis. *Chem. Rev.* **1995**, *95*, 759−788.

(2) Prins, R. Hydrogen Spillover. Facts and Fiction. *Chem. Rev.* **2012**, *112*, 2714−2738.

(3) Lueking, A.; Yang, R. T. Hydrogen Spillover from a Metal Oxide Catalyst onto Carbon Nanotubes—Implications for Hydrogen Storage. *J. Catal.* **2002**, *206*, 165−168.

(4) Lachawiec, A. J.; Qi, G.; Yang, R. T. Hydrogen Storage in Nanostructured Carbons by Spillover: Bridge-Building Enhancement. *Langmuir* **2005**, *21*, 11418−11424.

(5) Contescu, C. I.; Brown, C. M.; Liu, Y.; Bhat, V. V.; Gallego, N. C. Detection of Hydrogen Spillover in Palladium-Modified Activated Carbon Fibers during Hydrogen Adsorption. *J. Phys. Chem. C* **2009**, *113*, 5886−5890.

(6) Blackburn, J. L.; Engtrakul, C.; Bult, J. B.; Hurst, K.; Zhao, Y.; Xu, Q.; Parilla, P. A.; Simpson, L. J.; Rocha, J.-D. R.; Hudson, M. R.; Brown, C. M.; Gennett, T. Spectroscopic Identification of Hydrogen Spillover Species in Ruthenium-Modified High Surface Area Carbons by Diffuse Reflectance Infrared Fourier Transform Spectroscopy. *J. Phys. Chem. C* **2012**, *116*, 26744−26755.

(7) Liu, X. M.; Tang, Y.; Xu, E. S.; Fitzgibbons, T. C.; Larsen, G. S.; Gutierrez, H. R.; Tseng, H.-H.; Yu, M.-S.; Tsao, C.-S.; Badding, J. V.; Crespi, V. H.; Lueking, A. D. Evidence for Ambient-Temperature Reversible Catalytic Hydrogenation in Pt-doped Carbons. *Nano Lett.* **2013**, *13*, 137−141.

(8) Yang, F.; Hu, B.; Xia, W.; Peng, B.; Shen, J.; Muhler, M. On the nature of spillover hydrogen species on platinum/nitrogen-doped mesoporous carbon composites: A temperature-programmed nitrobenzene desorption study. *J. Catal.* **2018**, *365*, 55−62.

(9) Li, Q.; Lueking, A. D. Effect of Surface Oxygen Groups and Water on Hydrogen Spillover in Pt-Doped Activated Carbon. *J. Phys. Chem. C* **2011**, *115*, 4273−4282.

(10) Wang, L.; Yang, F. H.; Yang, R. T.; Miller, M. A. Effect of Surface Oxygen Groups in Carbons on Hydrogen Storage by Spillover. *Ind. Eng. Chem. Res.* **2009**, *48*, 2920−2926.

(11) Cheng, H.; Chen, L.; Cooper, A. C.; Sha, X.; Pez, G. P. Hydrogen spillover in the context of hydrogen storage using solid-state materials. *Energy Environ. Sci.* **2008**, *1*, 338−354.

(12) Wang, L.; Yang, R. T. Hydrogen Storage on Carbon-Based Adsorbents and Storage at Ambient Temperature by Hydrogen Spillover. *Catal. Rev.: Sci. Eng.* **2010**, *52*, 411−461.

(13) Warczinski, L.; Hu, B.; Eckhard, T.; Peng, B.; Muhler, M.; Hättig, C. Anchoring of palladium nanoparticles on N-doped mesoporous carbon. *Phys. Chem. Chem. Phys.* **2020**, *22*, 21317−21325.

(14) Granja-DelRío, A.; Alonso, J. A.; López, M. J. Steric and chemical effects on the hydrogen adsorption and dissociation on free and graphene-supported palladium clusters. *Comput. Theor. Chem.* **2017**, *1107*, 23−29.

(15) López-Corral, I.; Germán, E.; Juan, A.; Volpe, M. A.; Brizuela, G. P. DFT Study of Hydrogen Adsorption on Palladium Decorated Graphene. *J. Phys. Chem. C* **2011**, *115*, 4315−4323.

(16) Ramos-Castillo, C. M.; Reveles, J. U.; Zope, R. R.; de Coss, R. Palladium Clusters Supported on Graphene Monovacancies for Hydrogen Storage. *J. Phys. Chem. C* **2015**, *119*, 8402−8409.

(17) Rangel, E.; Sansores, E.; Vallejo, E.; Hernández-Hernández, A.; López-Pérez, P. A. Study of the interplay between N-graphene defects and small Pd clusters for enhanced hydrogen storage via a spill-over mechanism. *Phys. Chem. Chem. Phys.* **2016**, *18*, 33158−33170.

(18) Warczinski, L.; Hättig, C. A quantum chemical study of hydrogen adsorption on carbon-supported palladium clusters. *Phys. Chem. Chem. Phys.* **2019**, *21*, 21577−21587.

(19) Lueking, A. D.; Psofogiannakis, G.; Froudakis, G. E. Atomic Hydrogen Diffusion on Doped and Chemically Modified Graphene. *J. Phys. Chem. C* **2013**, *117*, 6312−6319.

(20) Sánchez, M.; Ruette, F. Calculations of adsorption, coadsorption, diffusion, and reaction barriers of H atoms in the H2 formation on a positively charged coronene. *Chem. Phys. Lett.* **2020**, *738*, 136913.

(21) Gerber, I. C.; Serp, P. A Theory/Experience Description of Support Effects in Carbon-Supported Catalysts. *Chem. Rev.* **2020**, *120*, 1250−1349.

(22) Hu, B.; Warczinski, L.; Li, X.; Lu, M.; Bitzer, J.; Heidelmann, M.; Eckhard, T.; Fu, Q.; Schulwitz, J.; Merko, M.; Li, M.; Kleist, W.; Hättig, C.; Muhler, M.; Peng, B. Formic Acid-Assisted Selective Hydrogenolysis of 5-Hydroxymethylfurfural to 2,5-Dimethylfuran over Bifunctional Pd Nanoparticles Supported on N-Doped Mesoporous Carbon. *Angew. Chem., Int. Ed.* **2021**, *60*, 6807−6815.
(23) Shamsiev, R. S.; Danilov, F. O. Quantum chemical study of H2 adsorption on Pd21 cluster. *Russ. Chem. Bull.* **2017**, *66*, 395−400.
(24) TURBOMOLE version 7.1, 2016; version 7.2.1 2017; and version 7.3, 2018; a development of University of Karlsruhe and Forschungszentrum Karlsruhe GmbH, 1989−2007, TURBOMOLE GmbH, since 2007. https://www.turbomole.com (2016−2018).
(25) Tao, J.; Perdew, J. P.; Staroverov, V. N.; Scuseria, G. E. Climbing the Density Functional Ladder: Nonempirical Meta−Generalized Gradient Approximation Designed for Molecules and Solids. *Phys. Rev. Lett.* **2003**, *91*, 146401.
(26) Weigend, F.; Ahlrichs, R. Balanced basis sets of split valence, triple zeta valence and quadruple zeta valence quality for H to Rn: Design and assessment of accuracy. *Phys. Chem. Chem. Phys.* **2005**, *7*, 3297−3305.
(27) Andrae, D.; Häußermann, U.; Dolg, M.; Stoll, H.; Preuß, H. Energy-adjustedab initio pseudopotentials for the second and third row transition elements. *Theor. Chim. Acta* **1990**, *77*, 123−141.
(28) Sierka, M.; Hogekamp, A.; Ahlrichs, R. Fast evaluation of the Coulomb potential for electron densities using multipole accelerated resolution of identity approximation. *J. Chem. Phys.* **2003**, *118*, 9136−9148.
(29) Weigend, F. Accurate Coulomb-fitting basis sets for H to Rn. *Phys. Chem. Chem. Phys.* **2006**, *8*, 1057−1065.
(30) Grimme, S.; Antony, J.; Ehrlich, S.; Krieg, H. A consistent and accurate ab initio parametrization of density functional dispersion correction (DFT-D) for the 94 elements H-Pu. *J. Chem. Phys.* **2010**, *132*, 154104.
(31) Koßmann, J.; Hättig, C. Investigation of interstitial hydrogen and related defects in ZnO. *Phys. Chem. Chem. Phys.* **2012**, *14*, 16392−16399.
(32) Stodt, D.; Noei, H.; Hättig, C.; Wang, Y. A combined experimental and computational study on the adsorption and reactions of NO on rutile TiO2. *Phys. Chem. Chem. Phys.* **2013**, *15*, 466−472.
(33) Plessow, P. Reaction Path Optimization without NEB Springs or Interpolation Algorithms. *J. Chem. Theory Comput.* **2013**, *9*, 1305−1310.
(34) Helgaker, T. Transition-state optimizations by trust-region image minimization. *Chem. Phys. Lett.* **1991**, *182*, 503−510.
(35) Fukui, K. The path of chemical reactions - the IRC approach. *Acc. Chem. Res.* **1981**, *14*, 363−368.
(36) Kesharwani, M. K.; Brauer, B.; Martin, J. M. L. Frequency and Zero-Point Vibrational Energy Scale Factors for Double-Hybrid Density Functionals (and Other Selected Methods): Can Anharmonic Force Fields Be Avoided? *J. Phys. Chem. A* **2015**, *119*, 1701−1714.
(37) Knizia, G. Intrinsic Atomic Orbitals: An Unbiased Bridge between Quantum Theory and Chemical Concepts. *J. Chem. Theory Comput.* **2013**, *9*, 4834−4843.
(38) Jewell, L. L.; Davis, B. H. Review of absorption and adsorption in the hydrogen−palladium system. *Appl. Catal., A* **2006**, *310*, 1−15.
(39) Blanco-Rey, M.; Juaristi, J. I.; Alducin, M.; López, M. J.; Alonso, J. A. Is Spillover Relevant for Hydrogen Adsorption and Storage in Porous Carbons Doped with Palladium Nanoparticles? *J. Phys. Chem. C* **2016**, *120*, 17357−17364.
(40) González-Herrero, H.; Cortes-del Río, E. C.; Mallet, P.; Veuillen, J.-Y.; Palacios, J. J.; Gómez-Rodríguez, J. M.; Brihuega, I.; Ynduráin, F. Hydrogen physisorption channel on graphene: a highway for atomic H diffusion. *2D Mater.* **2019**, *6*, 021004.
(41) Gokhale, A. A.; Kandoi, S.; Greeley, J. P.; Mavrikakis, M.; Dumesic, J. A. Molecular-level descriptions of surface chemistry in kinetic models using density functional theory. *Chem. Eng. Sci.* **2004**, *59*, 4679−4691.
(42) Psofogiannakis, G. M.; Froudakis, G. E. DFT Study of the Hydrogen Spillover Mechanism on Pt-Doped Graphite. *J. Phys. Chem. C* **2009**, *113*, 14908−14915.

https://doi.org/10.1021/acs.jpcc.0c11412
J. Phys. Chem. C XXXX, XXX, XXX−XXX